ToF-SIMS evaluation of calcium-containing silica/γ-PGA hybrid systems for bone regeneration

Daming Wang [a], **Jin Nakamura** [b], **Gowsihan Poologasundarampillai** [a], **Toshihiro Kasuga** [a], **Julian R. Jones** [a,*] and **David S. McPhail** [a,*]

[a] *Department of Materials, Imperial College London, South Kensington Campus, London, SW7 2AZ UK*
[b] *Department of Frontier Material, Graduate School of Engineering, Nagoya Institute of Technology, Gokiso-cho, Showa-ku, Nagoya, 466‑8555, Japan*

ABSTRACT

Inorganic/organic hybrids have great potential for the production of bioactive scaffolds which have tailored mechanical properties and degradation rates suitable for tissue engineering. For bone regeneration, calcium incorporation into hybrids at low temperatures is important due to its ability to stimulate new bone formation. As a consequence, understanding the homogeneity of the critical inorganic and organic components will be the key to the development of such hybrids. Therefore, the aim of this interdisciplinary study is to use Time-of-Flight Secondary Ion Mass Spectrometry (ToF-SIMS) to determine the homogeneity of these critical components. In this study we evaluate various sol-gel silica/γ-polyglutamic acid (γ-PGA) hybrids systems produced using different routes to introduce the calcium, thereby tailoring and optimizing hybrid syntheses and processing routes. Dimethyl carbonate (DMC) was invoked to improve the inorganic/organic coupling and its influence on the homogeneity in the process was also examined here. The results revealed that the calcium salt form of γ-PGA was promising for calcium incorporation since homogeneous products could be obtained. The ToF-SIMS data also indicated that the reaction time of hybrid synthesis and the timing of the addition of DMC can affect the homogeneity of hybrids.

Key words: ToF-SIMS, γ-polyglutamic acid, inorganic/organic hybrid, sol-gel process and calcium incorporation

1. Introduction

Bone is the second most implanted tissue in the human body after blood [1]. Over 2.2 million bone grafting procedures are performed worldwide annually, with autografts and allografts being the choice of graft materials [2]. Both materials have several problems and drawbacks hence synthetic bone regeneration constructs are actively being developed. An ideal synthetic bone graft must be bioactive that can induce and conduct bone cell ingrowth, and meanwhile should possess satisfactory mechanical properties and a tailorable degradation rate [3-7]. Many of the synthetic bone grafts are bioactive ceramics or glasses that can bond to bone, degrade in the body and stimulate osteogenesis, however they are brittle in nature and therefore are not tough enough for bone defect sites that are under cyclic loading [4, 7-9].

The creation of sol-gel inorganic/organic hybrids provides a strategy to soften bioactive ceramic/glasses by incorporating a degradable polymer. An inorganic/organic hybrid is different to a traditional composite material. In a hybrid the inorganic and organic components are not distinguishable above the sub-micron scale as they interact with each other via covalent coupling and form an interpenetrating network at the molecular level through the sol-gel process [7, 10]. Consequently, the hybrids have the potential to have excellent mechanical properties such as high toughness and different components can degrade congruently as one material [7, 10-17].

Various sol-gel hybrids have been developed with silica and polymers over last two decades [10, 14, 15, 18-26]. For bone regeneration, calcium incorporation into synthetic bone grafts is also an important step since calcium is vital for the formation of the hydroxycarbonate apatite (HCA) layer, which can work together with silicon to stimulate new bone tissue formation [6, 27-29]. However, it is challenging

to incorporate calcium effectively into a hybrid at low temperature. Calcium nitrate ($Ca(NO_3)_2$) is a widely-used calcium source for sol-gel bioactive glasses but toxic nitrate by-products can form during the synthesis [4, 30]. The removal of the by-products occurs above 600 ℃ and a temperature of 400 ℃ is required to incorporate calcium into the silica network [27, 28]. At such a high temperature, the polymer matrix of the inorganic/organic hybrids will be destroyed and thus other calcium sources and methods of introducing calcium at low temperature are needed.

As one of the polymers suitable for hybrid functionalization, γ-polyglutamic acid (γPGA) is a natural biopolymer which has been proved to be safe to the human body and can conduct enzymatic degradation [31, 32]. γ-PGA is found naturally in the free acid form and cannot be dissolved in water without any modification [32]. Recently, Poologasundarampillai *et al.* have fabricated calcium-containing silica/γPGA hybrids using the free acid form of γPGA with dimethylsulfoxide (DMSO) as the solvent and calcium chloride ($CaCl_2$), which has been used in several hybrid systems previously [14, 33-36], as the calcium source [14, 35]. However, γ-PGA can be made soluble in water by reacting it with $Ca(OH)_2$ to achieve the calcium salt form of the polymer. Valliant *et al.* introduced the calcium salt form of γPGA where γPGA can be water soluble in such a state and homogeneous silica/calcium-salt γ-PGA (γ-CaPGA) hybrids were obtained [29]. In both cases, glycidoxypropyltrimethoxy silane (GPTMS) was used for covalent coupling with the γ-PGA through the reaction between the open epoxy ring of the GPTMS and the carboxylic acid group of the γ-PGA [14, 29, 35]. Therefore, both of the hybrids fabricated by these two methods have a similar expected chemical structure (Fig. 1). However, the different use of the calcium sources and the solvents determined that the homogeneity of these hybrids can be affected, which may have an influence on the hybrid bioactivity efficiency and ion release. It was observed that for the DMSO samples the calcium was phase separated from the silica network since the components in hybrids cannot be homogenously dispersed in DMSO [14], whilst both silicon and calcium were evenly distributed throughout the hybrids when using the calcium salt form of γ-PGA [29], which is promising for calcium incorporation. To verify the observations mentioned above, further study is required on the homogeneity of these two hybrids synthesized with different solvents and ways to incorporate the calcium content.

In addition, a key aspect of the optimization of hybrids is to understand the uniformity of the critical elements (silicon, the inorganic network, and how calcium is present in the atomic structure) and the nature of any bonding between γPGA, the coupling agent (GPTMS) and the silica network within the hybrids. Time-of-flight secondary ion mass spectrometry (ToF-SIMS) is a powerful analytical technique in material science. ToF-SIMS can acquire the distribution of all the elements and even compounds in the periodic table from the top two atomic layers of the sample surface (high surface sensitivity) with trace element sensitivity (up to the range of ppb) [37-39]. Secondary ion maps can be obtained with high lateral resolution by using a primary ion beam to raster over the surface. Furthermore, by introducing a second ion source for etching the material a depth profile can be acquired to analyze the chemical information within the materials [37-41]. In addition, the development of cluster ion beams has enabled molecular depth profiling and excellent mass resolution i.e. exceeding 10,000 ($\Delta m/m$) also assists in distinguishing nominal same masses in the polymeric materials [42-47]. ToF-SIMS has been playing a critical role in biomaterial and biological fields.

In this paper, ToF-SIMS was applied to compare and evaluate various calcium-containing silica/γ-PGA hybrid systems: using the free acid form of γPGA dissolving in DMSO and using the soluble calcium salt form of γPGA as the polymer components, respectively. In addition, dimethyl carbonate (DMC) was attempted to enhance the calcium chelation ability and inorganic/organic coupling of silica/γ-CaPGA hybrids and its influence on the hybrid uniformity was also studied here: i) with different reaction time between GPTMS and γ-CaPGA i.e. 24, 48 and 72 hrs; ii) and with different timings of the addition of DMC i.e. adding DMC at the onset of and after the reactions mentioned above.

2. Materials and Methods

2.1. Synthesis of calcium-containing silica/γPGA hybrids

Poly γ-glutamic acid (γ-PGA) was purchased in the free acid powder form from Natto Biosciences, Canada and all other chemicals for the synthesis of various calcium-containing silica/γ-PGA hybrids were purchased from Sigma Aldrich, UK.

2.1.1. Hybrids using free acid form of γPGA as the polymer source

The calcium-containing silica/γ-PGA (40 wt% γ-PGA with 60 wt% inorganic composed of SiO_2 to CaO of 70 : 30 molar ratio) hybrid using DMSO as the solvent was synthesized using the two-pot reaction procedure described in the previous work [14]. Functionalization of γ-PGA with 3-glycidoxyproyltrimethoxysilane (GPTMS, the coupling agent) was carried out in DMSO with a molar ratio of GPTMS : γ-PGA of 2 for 12 h. The majority of the DMSO was removed from the reaction mixture using rotary vacuum evaporation. This was followed by the addition of $CaCl_2$ as the calcium source. The second pot was prepared by hydrolyzing tetraethyl orthosilicate (TEOS) in 1N HCl and water for 1 h. Finally the two mixtures, calcium containing functionalized γ-PGA and hydrolyzed sol were added together and allowed to react for 1 h. The hybrid precursor sol was then poured into Teflon molds which were sealed and left in an oven at 60 ℃ to gel. This was then aged and dried at 60 ℃ to obtain the final hybrid monoliths.

2.1.2. Using a calcium salt form of the γPGA as the polymer source

The calcium salt form of the silica/γ-PGA hybrid sol (Si/γ-CaPGA) was prepared by a variant of the synthesis procedure described previously [29]. 1.0 g of γ-PGA and 0.26 g of $Ca(OH)_2$ were mixed in 19 g of distilled water, followed by the addition of 0.92 g of GPTMS (the molar ratio of γ-PGA to GPTMS was 2). The mixture was allowed to react at room temperature to facilitate the covalent coupling between γ-CaPGA and GPTMS (the Crosslinking Step). The hybrid sol was then cast into cylindrical polymethyl propylene molds and tightly sealed. A temperature of 40 ℃ for 3 days was required for the gelling process and monolithic hybrid discs were obtained after drying for 10 days at 40 ℃.

2.1.3. Addition of dimethyl carbonate (DMC)

The preparation of DMC containing silica/γ-CaPGA hybrids followed the synthesis procedure described in Section 3.1.1.2 but with addition of 0.31 g of DMC to obtain a molar ratio of $Ca(OH)_2$ to DMC of 1. While in this case the molar ratio of GPTMS : DMC was 1.11 : 1. The influences of the length of the reaction time between γ-CaPGA and GPTMS and the timing of adding DMC on the homogeneity of hybrids were investigated here. The DMC was (a) added together with other components to produce the hybrid sol (termed Pre-addition) or (b) added separately after the crosslinking step, followed by 5 minutes of vigorous agitation (termed Post-addition). For the crosslinking step, the hybrid sols were stirred at room temperature for 24, 48 or 72 hours before the subsequent gelling and drying process.

2.2. ToF-SIMS evaluation of calcium-containing silica/γPGA hybrids

A ToF-SIMS instrument (TOF.SIMS 5, ION-TOF GmbH) was used to determine the homogeneity of various calcium-containing silica/γPGA hybrid systems. The notation used for the different hybrids is listed in Table 1. All the analyzed samples were ground and polished down to 4000 grit to obtain flat sample surfaces, followed by a drying process in a 40 ℃ oven to remove any moisture.

The detailed parameters used for the SIMS analyses can be found in Table 2. Prior to collecting any information a 10 keV C_{60}^+ cluster beam was used to eliminate the sample surface contaminant. Secondary ion maps of 256×256 pixels were constructed by using a 25 keV Bi_3^+ liquid metal ion source (Bi^+ beam for the hybrid using the solvent DMSO) with a cycle time of 100 µs. To investigate the change of the element/compound distribution with depth, a depth profile was generated following each secondary ion map scan by using the 10 keV C_{60}^+ beam to sputter the surface for 1s. A low-energy 20 eV electron gun was used for charge compensation with a 0.1s scan rate.

3. Results and Discussion

3.1. Hybrids using the free acid form of γPGA versus using the calcium salt form of γPGA

Fig. 2 shows the ToF-SIMS secondary ion maps of the silica/γ-PGA hybrid using DMSO as the solvent and $CaCl_2$ as the calcium source (here termed FA-γ-PGA) and the silica/γ-CaPGA hybrid using the calcium salt form of γ-PGA (termed S-γ-CaPGA herein), which can be used to understand the distribution of the critical elements and compounds within the materials. Si^+ (Fig. 2a and g, the matrix of the silica network) and $SiCH_3^+$ (Fig. 2b and h, the bond between the silica network and the coupling agent GPTMS) were chosen to represent the silica network. Fig. 2c and i shows the distribution of the overall calcium content in the hybrids whilst CaO_2^+ (Fig. 2d and j) and $CNCa^+$ (Fig. 2e and k) were used to be indicative of the calcium incorporated into the hybrids through the carboxylic group and the amine group from the γ-PGA, respectively (Fig. 1). CaO_2^+ can also be from the ionic bonding between calcium and the silica network. The distribution of γ-PGA was then examined through CH_2N^+ (Fig. 2f and l). For the FA-γ-PGA sample, CH_3SO^+ was observed (Fig. 2m), which may be from the incomplete evaporation of the DMSO residue, and $CaSO^+$ (Fig. 2n), which could be the calcium chelating with DMSO, was also be detected.

It was evident from the constant intensity of the images in Fig. 2a-f that all the species from S-γ-CaPGA, the hybrids using the calcium salt form of γ-PGA, were evenly distributed. This suggests that the calcium, the silica network and the γ-PGA were successfully incorporated into each other and formed interpenetrating networks. This was consistent with the observations in the previous work [29]. The homogeneous $CNCa^+$ implied another possibility, namely that the calcium can also be bonded to γ-PGA with the amine group in addition to the carboxylic group.

On examining the hybrids produced using the free acid form of γ-PGA dissolved in DMSO (FA-γ-PGA) it was clear that phase separation was occurring. Si^+ and $SiCH_3^+$ had a similar heterogeneous distribution, leaving the silicon-depleted areas at the lower part of the image, which were indicated by the red dashed lines (Fig. 2g and h). The overall calcium ion distribution looked homogenous (Fig. 2i); however, the other calcium-related species CaO_2^+ and $CNCa^+$ tended to aggregate on the top half of the ion maps (Fig. 2j and k, highlighted by the white dashed lines). The similar trend for CaO_2^+ and $CNCa^+$ implied that CaO_2^+ here should be indicative of the bonding between the calcium and the γ-PGA rather than the calcium chelating with the silica network. In any case calcium is not expected to enter the silicate network when calcium chloride is used as the calcium source, at least not unless high temperatures are used [28]. Fig. 2l shows that CH_2N^+, the possible γ-PGA identifier, was fairly evenly distributed but with a slightly enhanced signal around the top. By contrast, the depletion of CH_3SO^+ and $CaSO^+$ can be seen from the left top half of the image (Fig. 2m and n, highlighted by the blue dashed lines). It has been reported that calcium can chelate with DMSO if DMSO cannot be thoroughly removed [35]. Here, the similar distribution of CH_3SO^+ and $CaSO^+$ further demonstrated that the calcium can bond to both γ-PGA and DMSO in this hybrid.

From Fig. 2g-n it can be seen that all the species had a higher intensity close to the top part of the images except for CH_3SO^+ and $CaSO^+$ which had an inverse distribution. This suggested that the DMSO residue after the incomplete evaporation procedure expelled the other components and therefore significantly affected the homogeneity of the hybrids. An interesting observation was that the total Ca^+ signal was homogenous whilst CaO_2^+, $CNCa^+$ and $CaSO^+$ were not. In addition, both CaO_2^+ and $CNCa^+$ had an inverse distribution with respect to the $CaSO^+$. Therefore, the homogenous total Ca content could be derived from the calcium chelating with both γ-PGA and DMSO. For silicon species, a similar trend of Si^+ and $SiCH_3^+$ indicated that the silica network was successfully linked to the coupling agent GPTMS. The properties shown by Poologasundarampillai *et al.* indicated that γ-PGA can be coupled to the silica network through GPTMS [14, 35]. However, Valliant *et al.* indicated that the polymer was lost rapidly to solution, especially when the calcium salt form of γ-PGA was used [29]. The results here may provide an explanation in that CH_2N^+ had a different distribution from the silica network, suggesting that the

coupling degree between γ-PGA and the silica network was unsatisfactory i.e. γ-PGA only partially bonded to GPTMS.

Fig. 3 shows the depth profiles produced to investigate the distribution of all the mentioned components within the hybrids. The depth profiles of both hybrids had similar trends for the corresponding species and an unstable area can be seen from both of the profiles before the dashed line, which could be due to the well-known SIMS pre-equilibrium effect. In such an area the implantation of the atoms from the primary ion beam was changing the chemistry of the near sample surface until a stable state was reached. Furthermore surface contaminants can affect the ion yields and sputter rates at the beginning of the analysis. During the pre-equilibrium period the secondary ion yields and sputter yields continuously changed as the near-surface chemistry changed and it was very difficult to quantify the composition of the material. At steady state the rate of implantation of primary species is equal to the rate at which they are sputtered, and sputter rate and secondary ion yield are fixed (in a given matrix). In the stable areas all the calcium species (Ca^+, CaO_2^+ and $CNCa^+$) from both samples were constant whilst other species (Si^+, $SiCH_3^+$ and CH_2N^+) dropped and then leveled off. This implied that there was no change in composition with depth for all the components inside the hybrids. However, a higher silica content tended to accumulate on the outer part of the hybrids. The cause is still not clear. It has been shown that all the components were evenly distributed throughout the hybrid in a similar composition [29]. Therefore the sample presented in this thesis might be an individual case and more samples are needed for SIMS analysis to confirm this. It was worth pointing out that CH_3SO^+ and $CaSO^+$ also remained throughout the depth profile, suggesting that DMSO cannot be evaporated thoroughly and the evaporation procedure should be extended to obtain 'dryer and cleaner hybrids'. This also implies that the inhomogeneity could have been a result of the incomplete evaporation of DMSO.

The ToF-SIMS data revealed that the hybrids made in the presence of DMSO were not homogeneous, i.e. DMSO was not suitable for the sol-gel hybrid synthesis. In addition, compared to dissolving calcium chloride into the free acid form of γ-PGA, the results further demonstrated that using the calcium salt form of γ-PGA was promising for calcium incorporation and that homogeneous silica/γ-PGA hybrids can be obtained. However, the calcium incorporated in this way limits the maximum amount of calcium that can be incorporated in the hybrid since both calcium and GPTMS are bonded to the γ-PGA with the carboxylic groups [29]. The amount of bonding between the γ-PGA and GPTMS is therefore also limited. The SIMS results suggest that alternative processing routes or calcium sources are required to increase the calcium content in the hybrids while maintaining the homogeneity of the different constituents.

3.2. Silica/γ-CaPGA hybrids synthesized through ionic coupling using DMC

It is vital to obtain silica/γ-CaPGA hybrids with tailored calcium release for controlled delivery of calcium ions to stimulate bone cells. Introducing an anionic site such as a carboxylic group for ionic chelation of calcium is a simple route to enable calcium incorporation into a hybrid and subsequent to control calcium ion release. Previous studies reported by Valliant *et al.* [29] suggest that the nucleophilic reaction between the carboxylic groups of the γ-CaPGA and the epoxy ring of the GPTMS did not occur as well as expected. An alternative coupling mechanism is to use ionic crosslinking, as is used in the gelation of alginate hydrogels, i.e. calcium ions can chelate with carboxylic groups from adjacent molecules, forming an ionic linkage [48, 49]. Therefore, the hypothesis used by Nakamura *et al.* was that the GPTMS could be functionalized to replace the epoxy ring with a carboxylic acid group and could ionically crosslink with γ-CaPGA via calcium ions. Dimethyl carbonate (DMC) is a well-known volatile organic solvent consisting of a carbonyl group flanked by two methoxy groups. In the aqueous environment, DMC undergoes hydrolysis of the methoxy groups to produce carbonate species. The hydrolyzed DMC has the potential to bond with GPTMS through the formation of ester bonding and provide the carboxyl groups (DMC/GPTMS), thereby enabling GPTMS to ionically couple γ-CaPGA to produce a silica/ γ-CaPGA hybrid (Fig. 4).

DMC, however, shows little solubility in aqueous media before hydrolysis and therefore invokes phase separation during the synthesis of the silica/γ-CaPGA hybrid, leading to inhomogeneity in sample composition. Therefore, the timing of adding DMC during the synthesis must be carefully considered. Here, the aim was to investigate the influence of functionalizing GPTMS with DMC on the homogeneity of hybrids using ToF-SIMS analyses. Six different silica/γ-CaPGA hybrids were studied with different

reaction times between GPTMS and γ-CaPGA (24, 48 and 72 h) and with different timings for adding DMC i.e. at the onset of (Pre-addition) and after the reactions (Post-addition) mentioned above. The corresponding samples were termed S-24DMC$_{pre}$, S-24DMC$_{post}$, S-48DMC$_{pre}$, S-48DMC$_{post}$, S-72DMC$_{pre}$ and S-72DMC$_{post}$.

Fig. 5 shows the ToF-SIMS secondary ion maps for Si$^+$ and Ca$^+$ from the silica/γ-CaPGA hybrids synthesized with the different conditions mentioned above. It was apparent that the ion distribution of the Pre-addition samples (Fig. 5a-f) was quite different to that of the Post-addition samples (Fig. 5g-l). Precisely Si$^+$ and Ca$^+$ from the Pre-addition samples (Fig. 5a-d, S-24DMC$_{pre}$ and S-48DMC$_{pre}$) had a similar homogeneous distribution for each hybrid, only with some signal-depleted voids embedded. An exception from the Pre-addition samples was S-72DMC$_{pre}$ (Fig. 5e-f), in which a high concentration of Si chain-like areas were observed whilst there was no calcium signal in the same regions, suggesting that silicon-rich particles had formed. Similar observations were made for all the Post-addition samples (Fig. 5g-l) but with a relatively even Ca$^+$ distribution in S-24DMC$_{post}$ (Fig. 5h) and S-72DMC$_{post}$ (Fig. 5l). In addition, the Si$^+$ maps for the Post-addition samples revealed that the morphology of the silicon-rich particles varied with increasing reaction time between the GPTMS and the γ-CaPGA, from the aggregation of the silicon-rich blocks (Fig. 5g, S-24DMC$_{post}$) to the silicon-rich grids with evenly spread gaps (~50 μm) between each 'hole' (Fig. 5i, S-48DMC$_{post}$), and finally to the extremely dense silicon-rich nets with numerous tiny needle-like gaps (Fig. 5k, S-72DMC$_{post}$).

Fig. 6 provided a more detailed understanding of the silicon-rich/ calcium-depleted phenomenon in these four hybrids i.e. S-24DMC$_{post}$, S-48DMC$_{post}$, S-72DMC$_{post}$ and S-72DMC$_{pre}$. The distribution of the silica network was presented by the SiOH$^+$ maps (Fig. 6a, d, g and j) whilst CaO$^+$ represented the possible bonding between the calcium and the carboxylic group from γ-PGA and/or the carbonyl group from GPTMS (Fig. 6b, e, h and k). Compared to the Si$^+$ and Ca$^+$ maps, the silicon-rich/calcium-depleted phenomenon can be seen more clearly from the SiOH$^+$ and CaO$^+$ images and can be observed clearly from the overlay images of SiOH$^+$ and CaO$^+$ (Fig. 6c, f, i and l), especially for S-72DMC$_{post}$ (Fig. 6i) for which it was challenging to distinguish the difference in the Si$^+$ (Fig. 6g) and Ca$^+$ (Fig. 6h) images due to the tiny needle-like gaps. The calcium depletion was apparent from the CaO$^+$ maps for all the Post-addition samples (Fig. 6b, e and h) whilst their Ca$^+$ counterparts (Fig. 5h, j and l) were less characteristic. The Ca$^+$ image from S-72DMC$_{post}$ was very homogeneous (Fig. 5l). This indicated that the total Ca$^+$ maps do not represent the distribution of the calcium which chelated with the hybrids, probably because the degree of chelation was low and most of the calcium content was still in the form of calcium hydroxide rather than incorporated into either DMC/GPTMS or γ-PGA.

From Fig. 5 and Fig. 6 it can be inferred that homogenous silica/γ-CaPGA hybrids can be obtained if DMC was added at the onset of the reaction between GPTMS and γ-PGA (Pre-addition) whilst silicon-rich particles were produced when DMC was added after the formation of the GPTMS/γ-PGA sol (Post-addition). This may be due to the hydrophobicity of unhydrolyzed DMC and therefore the formation of DMC droplets. DMC was slightly soluble in aqueous media (~14 g/100 mL) and thus the sol in the sol-gel process without hydrolysis. However, GPTMS or its hydrolyzed form can be dissolved in DMC while the γ-CaPGA cannot. In the Pre-addition hybrid sol preparation, the DMC and other components were added together, enabling a sufficient reaction time for the DMC to be hydrolyzed thoroughly and to be dispersed evenly in the sol before the drying process. Therefore, homogeneous hybrids can be obtained in this way. In contrast, DMC was added to the hybrid sol without complete hydrolysis before drying in the Post-addition samples, leading to the formation of hydrophobic unhydrolyzed DMC droplets. As GPTMS was soluble in DMC droplets while γ-CaPGA can only be dissolved in the aqueous phase of the sol in this case, phase separation occurred between the unreacted GPTMS and γ-CaPGA. Silicon aggregates would then form with DMC, leaving the silicon-rich/calcium-depleted regions after the evaporation of DMC in the drying process. The exception is that the silicon-rich/calcium-depleted phenomenon also happened in S-72DMC$_{pre}$ and this may be because of the self-condensation of GPTMS to form silica clusters in the precursor sol during the 48~72 h reacting step.

To further demonstrate the silicon-rich/calcium-depleted phenomenon, the uniformity of GPTMS, γ-PGA and calcium and the influence of the timing of the addition of DMC on this uniformity were investigated (Fig. 7). SiC$_2$H$^+$ from GPTMS, CH$_2$N$^+$ from γ-PGA and CNCa$^+$ (the possible bonding between calcium and the amine group from γ-PGA) in S-24DMC$_{pre}$ and S-24DMC$_{post}$ were selected as the examples. All the ion distributions (Fig. 7a-c) were still homogeneous as with the Si$^+$ and Ca$^+$ maps

presented (Fig. 5a and b) in S-24DMC$_{pre}$. In addition, all the species were parallel and constant in the depth profile (Fig. 8a), suggesting the even dispersion of all the components throughout the Pre-addition hybrids. However, there were some signal-depleted areas (highlighted by the blue and red circles) in the CNCa$^+$ image (Fig. 7a) whilst the corresponding ion-rich regions formed in the same areas in the SiC$_2$H$^+$ (Fig. 7b with the blue circles) and CH$_2$N$^+$ maps (Fig. 7c with the red circles). This may imply that there was less incorporation of networks of DMC/GPTMS and γ-CaPGA in some regions.

In terms of the Post-addition hybrids, the silicon-rich/calcium-depleted phenomenon was clear from comparison of CNCa$^+$ (Fig. 7d) and SiC$_2$H$^+$ (Fig. 7e). CNCa$^+$ and SiC$_2$H$^+$ were indicative of γ-CaPGA and GPTMS, respectively. Therefore, the formation of the SiC$_2$H$^+$ rich regions was due to the aforementioned hypothesis that GPTMS dissolved in hydrophobic unhydrolyzed DMC droplets and remained as rich particles after the evaporation of DMC. Whereas γ-CaPGA was insoluble in DMC, thus γ-CaPGA was phase separated from the DMC-dissolving GPTMS particles, which was presented from the distribution of CNCa$^+$.

The CH$_2$N$^+$ distribution also suggested that the overall γ-PGA related content had a similar trend to the calcium-chelated components (Fig. 7f). From the depth profile it is clear that all the species experienced a slight decrease with depth except for Ca$^+$ and CaO$^+$ (Fig. 8b). The decrease of the silicon related content might originate the DMC/GPTMS droplets being brought to surface with the evaporation of the DMC during the drying process, resulting in higher concentration on the surface. However, an explanation of a decrease in the γ-PGA remains to be found. Further characterization of the surface chemical structure is needed to clarify this issue. It is worth noting that the distribution of CaO$^+$ (Fig. 6b) was similar to that of γ-PGA rather than GPTMS, implying that calcium tended to bond to the carboxylic groups from γ-PGA rather than to the carbonyl groups from the DMC/GPTMS. Therefore in the Post-addition samples, DMC may chelate with no or a lower amount of calcium. However, further analyses such as dissolution test and NMR are needed to confirm whether the ionic coupling occurs between the DMC and γ-CaPGA. Analysis of mechanical properties as a function of dissolution time for hybrids with and without DMC would also be of interest.

4. Conclusions

In this study the homogeneity of various calcium-containing silica/γ-PGA hybrid systems were investigated. The ToF-SIMS data revealed that the hybrids using the free acid form of γ-PGA with DMSO as the solvent were heterogeneous since the components in the hybrids could not be evenly dispersed in the presence of DMSO. This suggested that DMSO was not an ideal solvent for the sol-gel hybrid synthesis here. By contrast, using a calcium salt form of polymers was promising for calcium incorporation since homogeneous hybrids can be obtained through the sol-gel process in this way. Modification of GPTMS with DMC was attempted as an alternative coupling mechanism between the inorganic and organic networks and its influence on the uniformity of hybrid synthesis was examined. The results showed that the species could be evenly distributed when DMC was added with other components to the sol i.e. at the onset of the coupling reaction between GPTMS and γ-PGA. If DMC was added after the reaction without complete hydrolysis the silicon-rich/calcium-depleted phenomenon occurred. As a powerful chemical analysis technique, ToF-SIMS can provide a straightforward way of evaluating the performance of different materials, by studying the sample uniformity. It also demonstrates the feasibility of comparing various inorganic/organic hybrids, thereby optimizing the hybrid synthesis and processing routes.

References

[1] M. Geiger, R.H. Li, W. Friess, Collagen sponges for bone regeneration with rhBMP-2, Adv Drug Deliv Rev, 55 (2003) 1613-1629.
[2] US Market for Orthopedic Biomaterials, iData Research Report, 2010.
[3] P. Ducheyne, Q. Qiu, Bioactive ceramics: the effect of surface reactivity on bone formation and bone cell function, Biomaterials, 20 (1999) 2287-2303.
[4] J.R. Jones, L.M. Ehrenfried, L.L. Hench, Optimising bioactive glass scaffolds for bone tissue engineering, Biomaterials, 27 (2006) 964-973.
[5] J.R. Jones, New trends in bioactive scaffolds: The importance of nanostructure, Journal of the European Ceramic Society, 29 (2009) 1275-1281.
[6] L.L. Hench, J.M. Polak, Third-generation biomedical materials, Science, 295 (2002) 1014-1017.
[7] J.R. Jones, Review of bioactive glass: from Hench to hybrids, Acta Biomater, 9 (2013) 4457-4486.
[8] P. Sepulveda, J.R. Jones, L.L. Hench, Bioactive sol-gel foams for tissue repair, J Biomed Mater Res, 59 (2002) 340-348.
[9] L.L. Hench, The story of Bioglass, J Mater Sci Mater Med, 17 (2006) 967-978.
[10] O. Mahony, O. Tsigkou, C. Ionescu, C. Minelli, L. Ling, R. Hanly, M.E. Smith, M.M. Stevens, J.R. Jones, Silica-Gelatin Hybrids with Tailorable Degradation and Mechanical Properties for Tissue Regeneration, Advanced Functional Materials, 20 (2010) 3835-3845.
[11] E.M. Valliant, J.R. Jones, Softening bioactive glass for bone regeneration: sol-gel hybrid materials, Soft Matter, 7 (2011) 5083-5095.
[12] T. Niemela, H. Niiranen, M. Kellomaki, P. Tormala, Self-reinforced composites of bioabsorbable polymer and bioactive glass with different bioactive glass contents. Part I: Initial mechanical properties and bioactivity, Acta Biomater, 1 (2005) 235-242.
[13] K. Rezwan, Q.Z. Chen, J.J. Blaker, A.R. Boccaccini, Biodegradable and bioactive porous polymer/inorganic composite scaffolds for bone tissue engineering, Biomaterials, 27 (2006) 3413-3431.
[14] G. Poologasundarampillai, C. Ionescu, O. Tsigkou, M. Murugesan, R.G. Hill, M.M. Stevens, J.V. Hanna, M.E. Smith, J.R. Jones, Synthesis of bioactive class II poly(γ-glutamic acid)/silica hybrids for bone regeneration, Journal of Materials Chemistry, 20 (2010) 8952-8961.
[15] D. Tian, P. Dubois, R. Jerome, Biodegradable and biocompatible inorganic-organic hybrid materials .1. Synthesis and characterization, Journal of Polymer Science Part A: Polymer Chemistry, 35 (1997) 2295-2309.
[16] M. Laridjani, Structural studies of ideal organic-inorganic nanocomposites by high resolution diffractometry and NMR spectroscopy techniques, Journal of Materials Science, 34 (1999) 5945-5953.
[17] B.M. Novak, Hybrid nanocomposite materials - between inorganic glasses and organic polymer, Adv Mater, 5 (1993) 422-433.
[18] Z. Ahmad, J.E. Mark, Polyimide-ceramic hybrid composites by the sol-gel route, Chemistry of Materials, 13 (2001) 3320-3330.
[19] U. Schubert, N. Husing, A. Lorenz, Hybrid inorganic/organic materials by sol-gel processing of organofunctional metal alkoxides, Chemistry of Materials, 7 (1995) 2010-2027.
[20] A.L. Douglas, J.S. Kenneth, Bridged polysilsesquioxanes. Highly porous hybrid organic/inorganic materials, Chemical Reviews, 95 (1995) 1431-1442.
[21] T. Ogoshi, Tomoki|Ogoshi,T,Tomoki, Synthesis of anionic polymer-silica hybrids by controlleing pH in an aqueous solution, Journal of Materials Chemistry, 15 (2005) 315-322.
[22] M.B. Novak, Hybrid nanocomposite materials - between inorganic glasses and organic polymer, Advanced Materials, 5 (1993) 422-433.
[23] Y. Shirosaki, T. Okayama, K. Tsuru, S. Hayakawa, A. Osaka, Synthesis and cytocompatibility of porous chitosan-silicate hybrids for tissue engineering scaffold application, Chemical Engineering Journal, 137 (2008) 122-128.
[24] L. Ren, K. Tsuru, S. Hayakawa, A. Osaka, Sol-gel preparation and in vitro deposition of apatite on porous gelatin-siloxane hybrids, Journal of Non-Crystalline Solids, 285 (2001) 116-122.
[25] L. Ren, K. Tsuru, S. Hayakawa, A. Osaka, Novel approach to fabricate porous gelatin-siloxane hybrids for bone tissue engineering, Biomaterials, 23 (2002) 4765-4773.
[26] Y. Shirosaki, K. Tsuru, S. Hayakawa, A. Osaka, M.A. Lopes, J.D. Santos, M.H. Fernandes, In vitro cytocompatibility of MG63 cells on chitosan-organosiloxane hybrid membranes, Biomaterials, 26 (2005) 485-493.
[27] S. Lin, C. Ionescu, S. Baker, M.E. Smith, J.R. Jones, Characterisation of the inhomogeneity of sol–gel-derived SiO2–CaO bioactive glass and a strategy for its improvement, Journal of Sol-Gel Science and Technology, 53 (2009) 255-262.
[28] B. Yu, C.A. Turdean-Ionescu, R.A. Martin, R.J. Newport, J.V. Hanna, M.E. Smith, J.R. Jones, Effect of calcium source on structure and properties of sol-gel derived bioactive glasses, Langmuir, 28 (2012) 17465-17476.
[29] E.M. Valliant, F. Romer, D. Wang, D.S. McPhail, M.E. Smith, J.V. Hanna, J.R. Jones, Bioactivity in silica/poly(gamma-glutamic acid) sol-gel hybrids through calcium chelation, Acta Biomater, 9 (2013) 7662-7671.
[30] S. Lin, C. Ionescu, K.J. Pike, M.E. Smith, J.R. Jones, Nanostructure evolution and calcium distribution in sol-gel derived bioactive glass, Journal of Materials Chemistry, 19 (2009) 1276-1282.
[31] L.R. Lake, Carbohydrase and Protease Enzyme Preparations Derived From Bacillus Subtilis or Bacillus Amyloliquefaciens; Affirmation of GRAS Status as Direct Food Ingredients, in, Department of Health and Human Services, 1999, pp. 19887-19895.
[32] G.-H. Ho, T.-I. Ho, K.-H. Hsieh, Y.-C. Su, P.-Y. Lin, J. Yang, K.-H. Yang, S.-C. Yang, γ-Polyglutamic acid produced by bacillus subtilis (natto): structural characteristics, chemical properties and biological functionalities, Journal of the Chinese Chemical Society, 53 (2006) 1363-1384.

[33] B.A. Allo, A.S. Rizkalla, K. Mequanint, Synthesis and electrospinning of ε-polycaprolactone-bioactive glass hybrid biomaterials via a sol− gel process, Langmuir, 26 (2010) 18340-18348.

[34] M.M. Pereira, J.R. Jones, L.L. Hench, Bioactive glass and hybrid scaffolds prepared by sol–gel method for bone tissue engineering, Advances in Applied Ceramics, 104 (2005) 35-42.

[35] G. Poologasundarampillai, B. Yu, O. Tsigkou, E. Valliant, S. Yue, P.D. Lee, R.W. Hamilton, M.M. Stevens, T. Kasuga, J.R. Jones, Bioactive silica–poly(γ-glutamic acid) hybrids for bone regeneration: effect of covalent coupling on dissolution and mechanical properties and fabrication of porous scaffolds, Soft Matter, 8 (2012) 4822.

[36] Y. Shirosaki, K. Tsuru, S. Hayakawa, A. Osaka, M.A. Lopes, J.D. Santos, M.H. Fernandes, In vitro cytocompatibility of MG63 cells on chitosan-organosiloxane hybrid membranes, Biomaterials, 26 (2005) 485-493.

[37] J.C. Vickerman, I. Gilmore, Surface analysis: the principal techniques, John Wiley & Sons Inc, US, 2009.

[38] D.S. McPhail, Applications of Secondary Ion Mass Spectrometry (SIMS) in Materials Science, Journal of Materials Science, 41 (2006) 873-903.

[39] J.C. Vickerman, D. Briggs, ToF-SIMS: Surface Analysis by Mass Spectrometry, IM Publications LLP UK, 2001.

[40] A.M. Belu, D.J. Graham, D.G. Castner, Time-of-flight secondary ion mass spectrometry: techniques and applications for the characterization of biomaterial surfaces, Biomaterials, 24 (2003) 3635-3653.

[41] R.N. Sodhi, Time-of-flight secondary ion mass spectrometry (TOF-SIMS): versatility in chemical and imaging surface analysis, The Analyst, 129 (2004) 483-487.

[42] N.M. Reed, J.C. Vickerman, The application of static secondaryion mass spectrometry (SIMS) to the surface analysis of polymermaterials, in: L. Sabbatini, P.G. Zambonin (Eds.) Surface characterization of advanced polymers, VCH, Weinheim, Germany, 1993.

[43] C.M. Mahoney, Cluster secondary ion mass spectrometry of polymers and related materials, Mass Spectrom Rev, 29 (2010) 247-293.

[44] G. Gillen, S. Roberson, Preliminary evaluation of an SF5+ polyatomic primary ion beam for analysis of organic thin films by secondary ion mass spectrometry, Rapid Commun Mass Sp, 12 (1998) 1303-1312.

[45] A. Brunelle, D. Touboul, O. Laprevote, Biological tissue imaging with time-of-flight secondary ion mass spectrometry and cluster ion sources, J Mass Spectrom, 40 (2005) 985-999.

[46] N. Winograd, The magic of cluster SIMS, Anal Chem, 77 (2005) 143A-149A.

[47] A. Wucher, Molecular secondary ion formation under cluster bombardment: A fundamental review, Appl Surf Sci, 252 (2006) 6482-6489.

[48] C.K. Kuo, P.X. Ma, Ionically crosslinked alginate hydrogels as scaffolds for tissue engineering: Part 1. Structure, gelation rate and mechanical properties, Biomaterials, 22 (2001) 511-521.

[49] Y.-H. Lin, H.-F. Liang, C.-K. Chung, M.-C. Chen, H.-W. Sung, Physically crosslinked alginate/N,O-carboxymethyl chitosan hydrogels with calcium for oral delivery of protein drugs, Biomaterials, 26 (2005) 2105-2113.

Table 1 Denotation of various calcium-containing silica/ γ-PGA hybrids. The molar ratio of γ-PGA to GPTMS (GC) was 2 in all the samples.

Sample	Solvent	Calcium source	PGA form	Reaction time between γ-PGA and GPTMS	Timing of adding DMC
FA-γ-PGA	DMSO	CaCl$_2$	free acid	12h	-
S-γ-CaPGA				48h	-
S-24DMC$_{pre}$				24h	Pre-addition
S-24DMC$_{post}$					Post-addition
S-48DMC$_{pre}$	Water	Ca(OH)$_2$	salt form	48h	Pre-addition
S-48DMC$_{post}$					Post-addition
S-72DMC$_{pre}$				72h	Pre-addition
S-72DMC$_{post}$					Post-addition

Table 2 Parameters for the SIMS analyses on various calcium-containing silica/ γ-PGA hybrids.

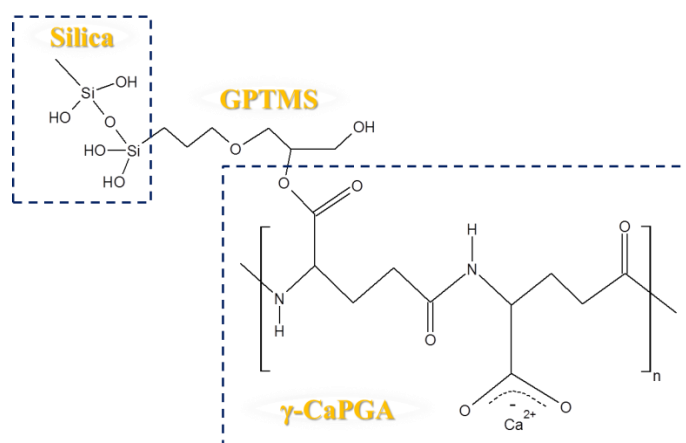| Sample	Analysis beam	Analysis area (μm^2)	Sputter beam	Sputtered area (μm^2)	Number of scans
FA-γ-PGA	Bi$^+$ ~1.2 pA	100 × 100		~0.6 nA	250 × 250	
S-γ-CaPGA		300 × 300		~0.6 nA	500 × 500	
S-24DMC$_{pre}$		500 × 500		~1.2 nA	700 × 700	
S-24DMC$_{post}$		300 × 300	C$_{60}^+$	~0.6 nA	500 × 500	400
S-48DMC$_{pre}$	Bi$_3^+$ ~0.6 pA	500 × 500		~1.6 nA	700 × 700	
S-48DMC$_{post}$		300 × 300		~0.6 nA	500 × 500	
S-72DMC$_{pre}$		300 × 300		~1 nA	500 × 500	
S-72DMC$_{post}$		500 × 500		~0.6 nA	700 × 700	

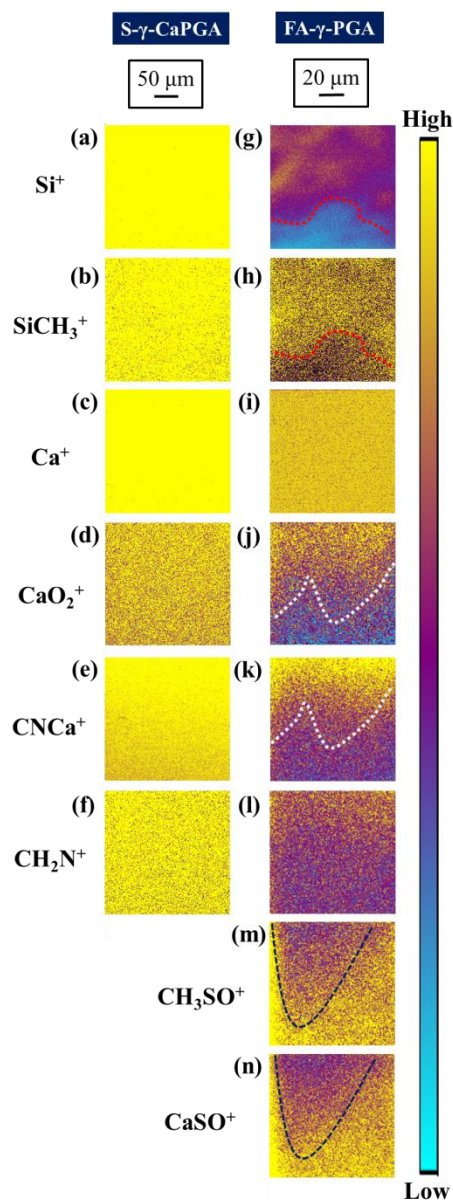Fig. 1 Schematic for the expected structure of the calcium-containing silica/γ-PGA hybrid.

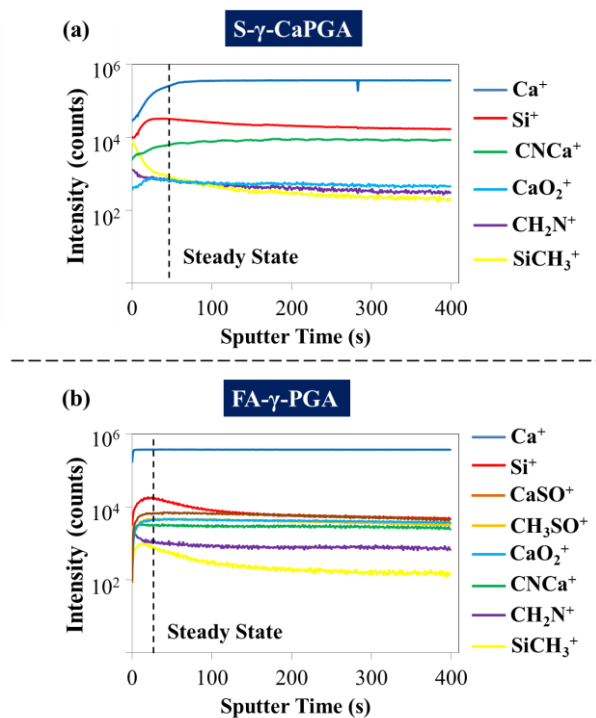Fig. 2   ToF-SIMS secondary ion mapping for the calcium-containing silica/γ-PGA hybrids synthesized with (a-f) the calcium salt form of γ-PGA (S-γ-CaPGA) and with (g-m) the free acid form of γ-PGA using DMSO as the solvent (FA-γ-PGA). The distribution of the critical elements and compounds were investigated as follows: (a) (g) Si^+; (b) (h) $SiCH_3^+$; (c) (i) Ca^+; (d) (j) CaO_2^+; (e) (k) $CNCa^+$; (f) (l) CH_2N^+; (m) CH_3SO^+ and (n) $CaSO^+$. The scale bars are 50 μm for S-γ-CaPGA and 20 μm for FA-γ-PGA.

Fig. 3　ToF-SIMS Depth profiles of the calcium-containing silica/γ-PGA hybrids synthesized with (a) the calcium salt form of γ-PGA (S-γ-CaPGA) and with (b) the free acid form of γ-PGA using DMSO as the solvent (FA-γ-PGA). The intensity of the critical ions from both hybrids with sputter time was shown.
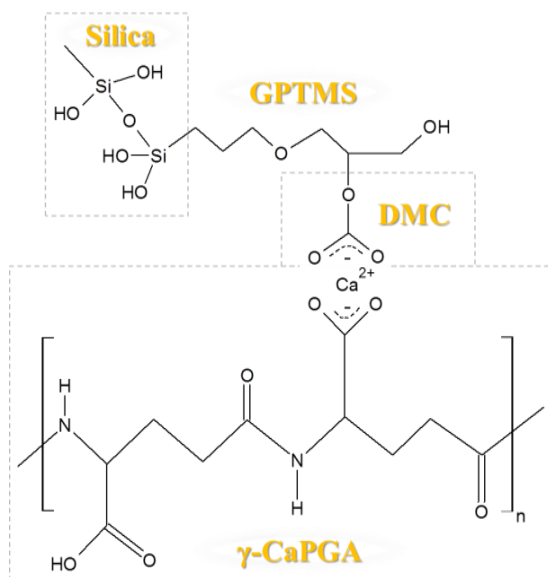
Fig. 4　Schematic for the expected structure of a silica/γ-CaPGA hybrid synthesized through the ionic coupling between the hydrolyzed DMC-coupled GPTMS (DMC/GPTMS) and γ-CaPGA.
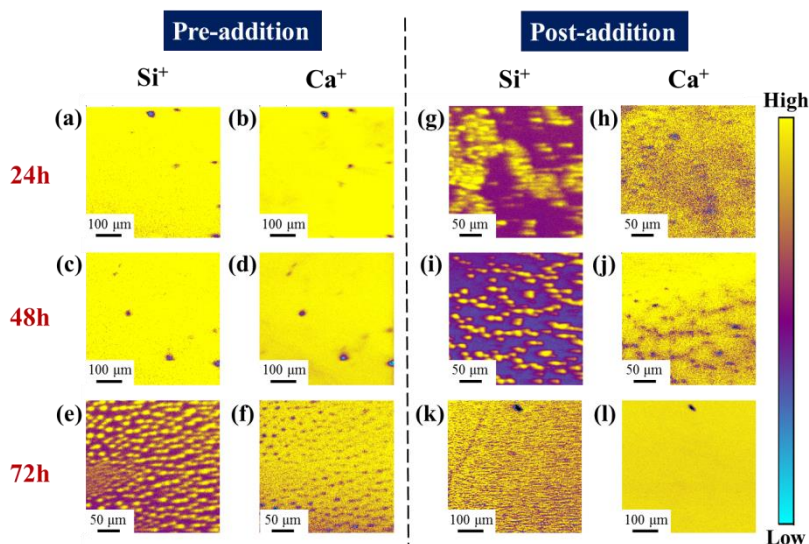
Fig. 5   ToF-SIMS secondary ion maps of Si$^+$ and Ca$^+$ for the silica/γ-CaPGA hybrids with the addition of DMC (a-f) at the onset of the reaction between GPTMS and γ-CaPGA and (g-l) after the reaction. Various reaction times between GPTMS and γ-CaPGA were studied here with (a) (b) (g) (h) 24 h; (c) (d) (i) (j) 48 h and (e) (f) (k) (l) 72 h.
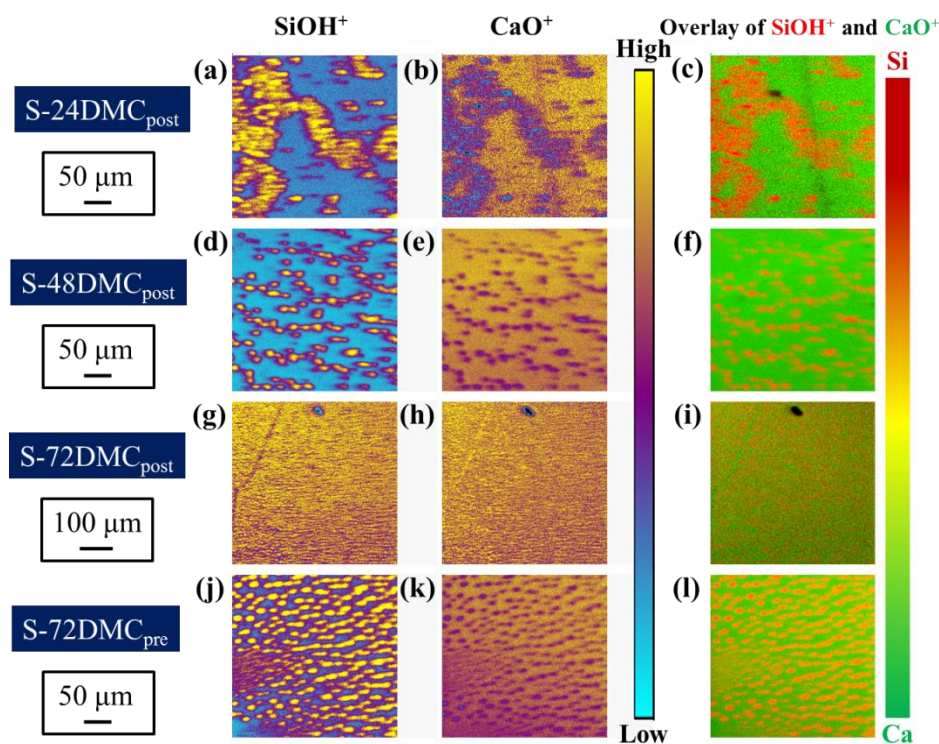

Fig. 6   ToF-SIMS analysis of the silica/γ-CaPGA hybrids with the addition of DMC: (a-i) after the reaction between GPTMS and γ-CaPGA (S-xDMC$_{post}$) and (j-l) at the onset of the reaction (S-xDMC$_{pre}$). x = 24, 48 or 72, referring to the different reaction time between GPTMS and γ-CaPGA with 24 h, 48 h and 72 h. The distribution of SiOH$^+$ and CaO$^+$ and the overlay images of SiOH$^+$ (red) and CaO$^+$ (green) were shown from (a) (b) (c) S-24DMC$_{post}$; (e) (f) (g) S-48DMC$_{post}$; (e) (f) (g) S-72DMC$_{post}$ and (e) (f) (g) S-72DMC$_{pre}$. The scale bars are 50 μm for S-24DMC$_{post}$, S-48DMC$_{post}$, S-72DMC$_{pre}$ and 100 μm for S-72DMC$_{post}$.
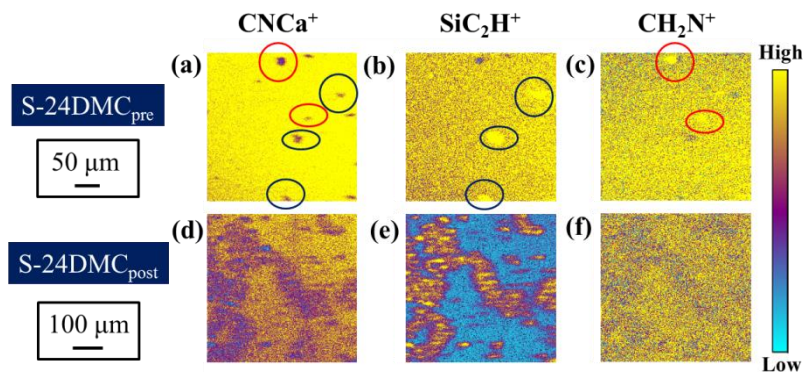
Fig. 7 ToF-SIMS analysis of the DMC-containing silica/γ-CaPGA hybrids synthesized with the 24 h reaction between GPTMS and γ-CaPGA. The data were obtained from the hybrids with the addition of DMC: (a-c) at the onset of the 24 h reaction (S-24DMC$_{pre}$) and (d-f) after the 24 h reaction (S-24DMC$_{post}$). Secondary ion maps showed the distribution of CNCa$^+$, SiC$_2$H$^+$ and CH$_2$N$^+$. The scale bars are 50 μm for S-24DMC$_{post}$ and 100 μm for S-24DMC$_{post}$.
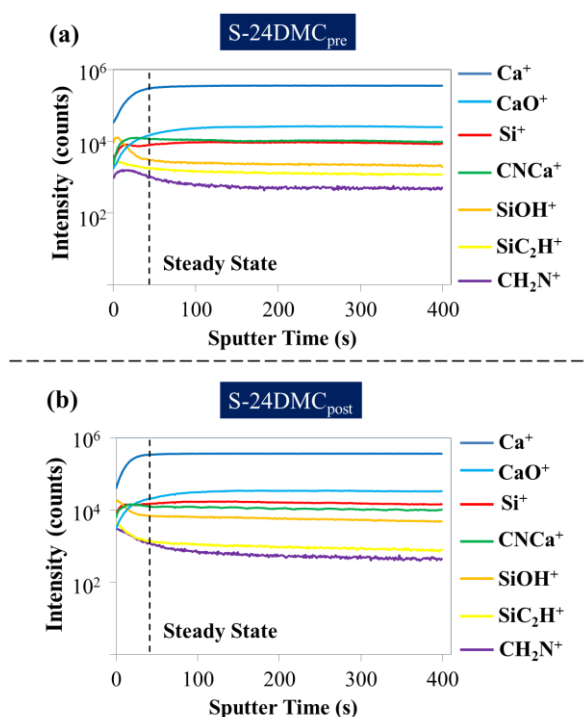

Fig. 8 ToF-SIMS depth profiles of the silica/γ-CaPGA hybrids with the addition of DMC: (a) at the onset of the 24 h reaction (S-24DMC$_{pre}$) between GPTMS and γ-CaPGA, and (b) after the 24 h reaction (S-24DMC$_{post}$). The intensity of the critical ions from both hybrids with sputter time was shown.